Wide area Raman spectroscopy

Wide area Raman spectroscopy

Andrew Downes

School of Engineering, Institute for Bioengineering, University of Edinburgh, Edinburgh, UK

Abstract:

Raman spectroscopy allows non-destructive analysis of materials using laser illumination. However, most Raman spectrometers can only provide good signal levels and sufficient spectral resolution, by focusing the laser to micrometer-sized spots. This equates to enormous laser intensities, which for samples with even very minor optical absorption either means destroying or damaging it by absorbing even a tiny fraction of the laser power, or it means reducing the laser intensity and hence the signal level. Furthermore, Raman signals generated above or below the focal plane are rejected in traditional Raman spectrometers. As signal levels are already extremely low in Raman spectroscopy, several schemes offer an alternative to focussing down to a diffraction-limited spot, to increase the area by up to 6 orders of magnitude, and increase the sampling depth. This review describes and compares these schemes, and estimates the typical illumination areas.

1. Introduction to Raman spectroscopy

When laser light of a well-defined frequency is incident onto a molecule or crystalline material, it can lose energy to excite a vibration within the molecule or crystal. After interaction with the material, some of the detected photons are red-shifted, and the frequency shift is equal to the frequency of vibration. Hence, from analysing the red-shifted light we can measure a spectrum of vibrational frequencies which relates to the material investigated by the laser. This effect was discovered by C.V. Raman [1], for which the Nobel prize was awarded, and we now refer to as Raman spectroscopy.

Raman spectroscopy has been applied to solids, liquids and gases [2-4], but the number of collected photons is small – due to the weak efficiency of Raman scattering, with typically only 1 in 10^8 – 10^{10} photons red-shifted. As a result, acquisition times of 1 – 10 seconds are typical for spectroscopy of solids and liquids when using the full available laser power. Example Raman spectra are shown in Figure 1, for a variety of solvents. The frequency shift is displayed in units of cm^{-1}, and widths of spectral peaks can be broadened by the spectrometer to around 10 cm^{-1}, but this is still sufficient to distinguish the liquids based on their characteristic vibrational frequencies. Although many investigations such as in gases require far higher spectral resolution, 10 cm^{-1} is normally sufficient to perform materials analysis.

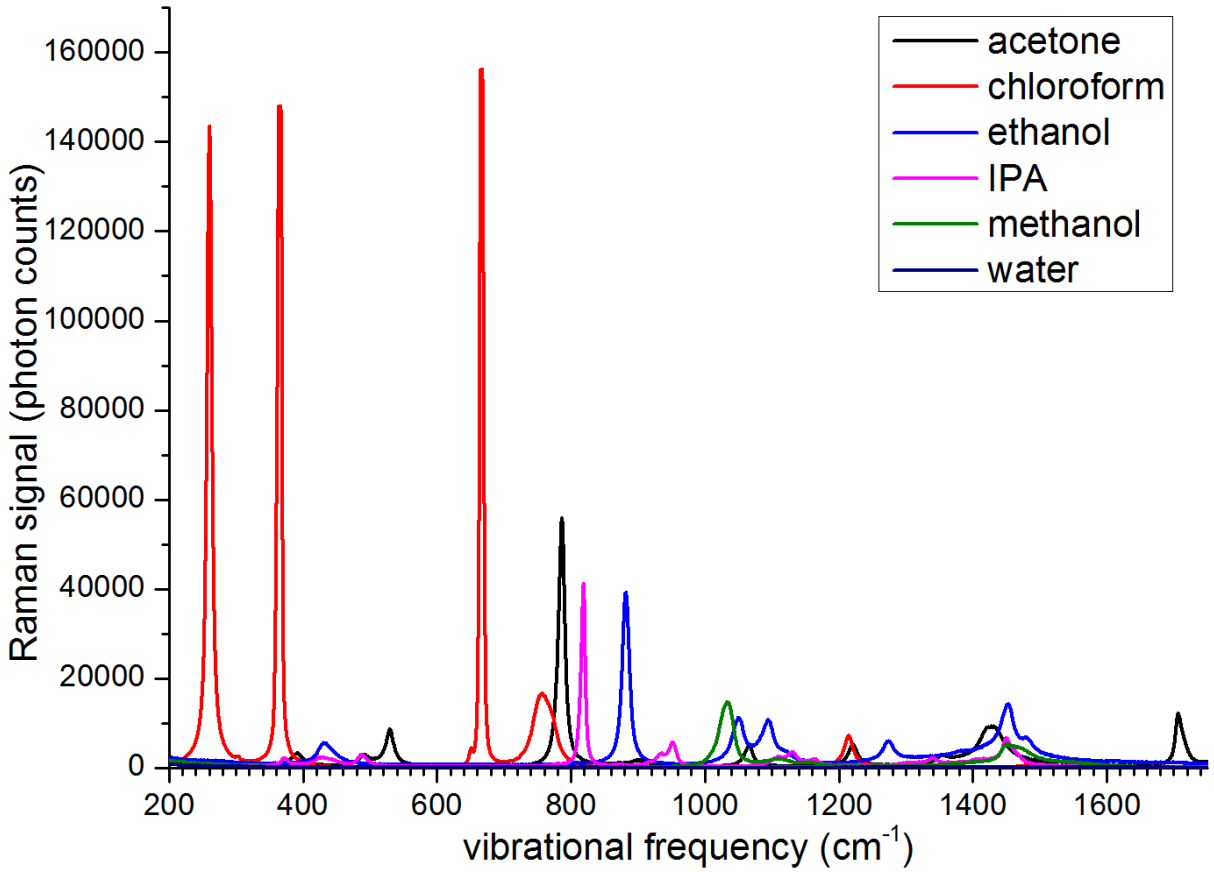

Figure 1. Raman spectra of various liquids. Each liquid has a clearly identifiable spectrum, and spectral widths vary from around 8 cm^{-1} (limited by the spectrometer resolution) to over 20 cm^{-1} (governed by the natural linewidth of the vibrations). A laser wavelength of 785 nm was used, focused into a spot within each liquid between quartz coverslips, in a Renishaw InVia Raman spectrometer. The acquisition time was 10 s and 50 mW of laser power was focused into the sample using a 50x objective lens with 0.75 NA. Saturation of the CCD detector has occurred for the three largest peaks in chloroform.

Most Raman spectrometers employ a diffraction grating to disperse the red-shifted light, and a CCD camera to count individual photons after they have been dispersed into a spectrum. This is depicted in Figure 2(A), where a laser is focused to a spot of size 0.5 – 15 µm in diameter. Given the available laser powers for narrowband lasers suitable for Raman (e.g. 500 mW for 785 nm), it is clear that many materials will be heated or damaged by such high laser intensities (of the order 10^8 W cm^{-2}, which is 4 orders of magnitude higher than at the surface of the sun). Such intensities are far above the limits for human exposure (295 mW cm^{-2} for 785 nm), but can be employed on samples where absorption is extremely low, such as human cells cultured *in vitro*. However, for many materials absorption of laser light is sufficient to cause heating. In these cases laser powers need to be reduced by orders of magnitude to avoid damage, which means that signal levels in Raman spectra are also reduced by orders of magnitude compared to what could be acquired with the full laser power. There is therefore a need to address the issue of low Raman signals from this class of materials which have even a modest optical absorption co-efficient at the laser wavelength, and hence can only permit extremely low laser intensities. Solving this requires illuminating a large area with the full laser power laser – ideally around a square centimeter – and collecting the Raman signal from this large region. Brain tissue, which has a very low absorption coefficient of around 0.05 mm^{-1} for grey matter [5], was heated by a

fraction of a degree using laser intensities of 200 - 600 mW mm^{-2} for a wavelength of 638 nm [6]. This suggests that any material with an absorption length of 20 mm requires an area of illumination of the order of 1 mm^2 to prevent the sample heating by one degree. As well as allowing the full laser power to be used, illuminating over a large area will also allow more signal to be collected from a larger depth within the sample of interest, thereby increasing signal levels compared to the shallow depth of field achieved when focussing the laser into a diffraction-limited spot.

Some materials have high scattering coefficients, such as bone or brain tissue, so even if absorption coefficients are low (so that high laser intensities can be used), most of the signal generated by light after scattering below the surface does not make it through the spectrometer slit. Hence there is also a need in highly scattering materials to collect from a large area and depth. In addition, many samples have high heterogeneity so would give extremely variable Raman spectra depending on where exactly a small focused spot was positioned. In these cases (such as food, cancerous tissue, and artworks) a single spectrum acquired from a large area is strongly preferred to averaging a large number of spectral acquisitions from different locations, and could avoid the time and cost required to focus a spot onto a feature at the sample's surface using a microscope arrangement.

In this review, a number of alternative schemes will be described, to detect Raman signals from larger areas than a 15 µm diameter focused spot. All these schemes will be compared to the traditional method of spot illumination shown in Fig 2(A), in terms of the area of illumination and detection. For a given laser intensity, the expected signal levels between all schemes are compared, for available optics components. However, the gain from an increased collection depth is not included, as this depends strongly on the coefficients of absorption and scattering for the sample material. Before this comparison of wide area detection schemes in section 3, section 2 describes the trade-offs between collection area and either spectral resolution or numerical aperture, in traditional Raman spectroscopy with a focused spot.

2. Trade-offs: collection area vs. spectral resolution, and collection area vs. numerical aperture

For a traditional Raman spectrometer as depicted in Figure 2(A), it is clear that if the laser spot size is increased, and the slit is removed or has its width increased, the width of a given peak will increase. This is because the red or green spot will increase in size on the CCD detector and produce blurring along the wavelength axis of the CCD chip. The spectral resolution is approximated by [7] $\delta\lambda \approx \frac{RF \cdot \Delta\lambda \cdot W_S}{n \cdot W_P}$ where $\Delta\lambda$ is the wavelength range dispersed across the CCD detector, n is the number of pixels on the detector, W_S is the slit width, and W_P is the pixel width on the detector. RF is the resolution factor, which is equal to 1.5 when $W_S >> W_P$. For a common CCD detector optimised for spectroscopy n is 1600, and W_P is 16 µm. For a slit width of 100 µm and wavelength range of 100 nm, this gives rise to a spectral resolution $\delta\lambda$ of 0.6 nm. This translates to a spectral width of around 10 cm^{-1}, which is sufficient for identification of materials from their Raman spectra. So we will take 100 µm as a typical slit width, although an optical fiber of diameter 105 µm would give rise to a similar spectral resolution as a slit. For a laser wavelength of 785 nm, a wavelength range of 100 nm on the detector is equivalent to a wavenumber range across the detector of between 1000 and 1400 cm^{-1}, which is sufficient for identification of the vast majority of materials.

Many spectrometers used for Raman analysis have a focal length close to 0.25 m and have f/ numbers of up to f/2, which relates to an acceptance angle of ±14°, or a numerical aperture (sine of this angle) of 0.24. A numerical aperture of 0.2 is chosen here as a typical value of a good spectrometer. This

means that if an objective lens is chosen with the same numerical aperture, a spot size of 100 µm will map 1:1 from the sample to the CCD detector. The magnification of the spot from the sample to the detector is given by the ratio of the numerical apertures of the objective lens and the spectrometer: magnification M = NA(collection)/NA(spectrometer). Using a high numerical aperture objective lens (1.4 oil immersion) and a spectrometer of NA 0.2, this means that the laser spot on the sample has been magnified by a factor of 7. This relates to a spot on the sample of diameter 100 µm / 7, or around 15 µm. If the laser beam fills the aperture at the rear of a 1.4 NA objective lens, the spot size will be close to the theoretical diffraction-limited value of around half the wavelength. In order to increase the spot size, the beam diameter can be reduced ('underfilling' the objective lens), or the beam can be slightly diverging or converging, so focusses to a plane above or below the surface of the sample. Either method would create the required 15 µm diameter spot on the sample surface.

For a constant laser power, and a sample with very low absorption or scattering, a high numerical aperture lens should be used to collect as much isotropically emitted Raman signal as possible from the possible range of angles. However, when a sample with significant absorption or scattering is used, a different regime is in place: for a constant laser intensity (in mW cm^{-2}) on the sample to prevent damage, the signal level is proportional to the area from which light is collected on the sample, and is also proportional to the solid angle of collection (which is approximated roughly by the square of the numerical aperture). So in this case a large spot and small numerical aperture of collection (100 µm diameter and NA = 0.2) will gather as much signal as a small spot with a high numerical aperture of collection (15 µm diameter and NA = 1.4). It is therefore not possible to have both a large angle of collection (NA up to 1.4) and a large spot diameter, when a constant laser intensity is focused onto the sample. The product of NA^2 and area of collection (on the sample) is invariant, and this product is used to numerically compare the throughput of the various wide area Raman schemes, later in table 1.

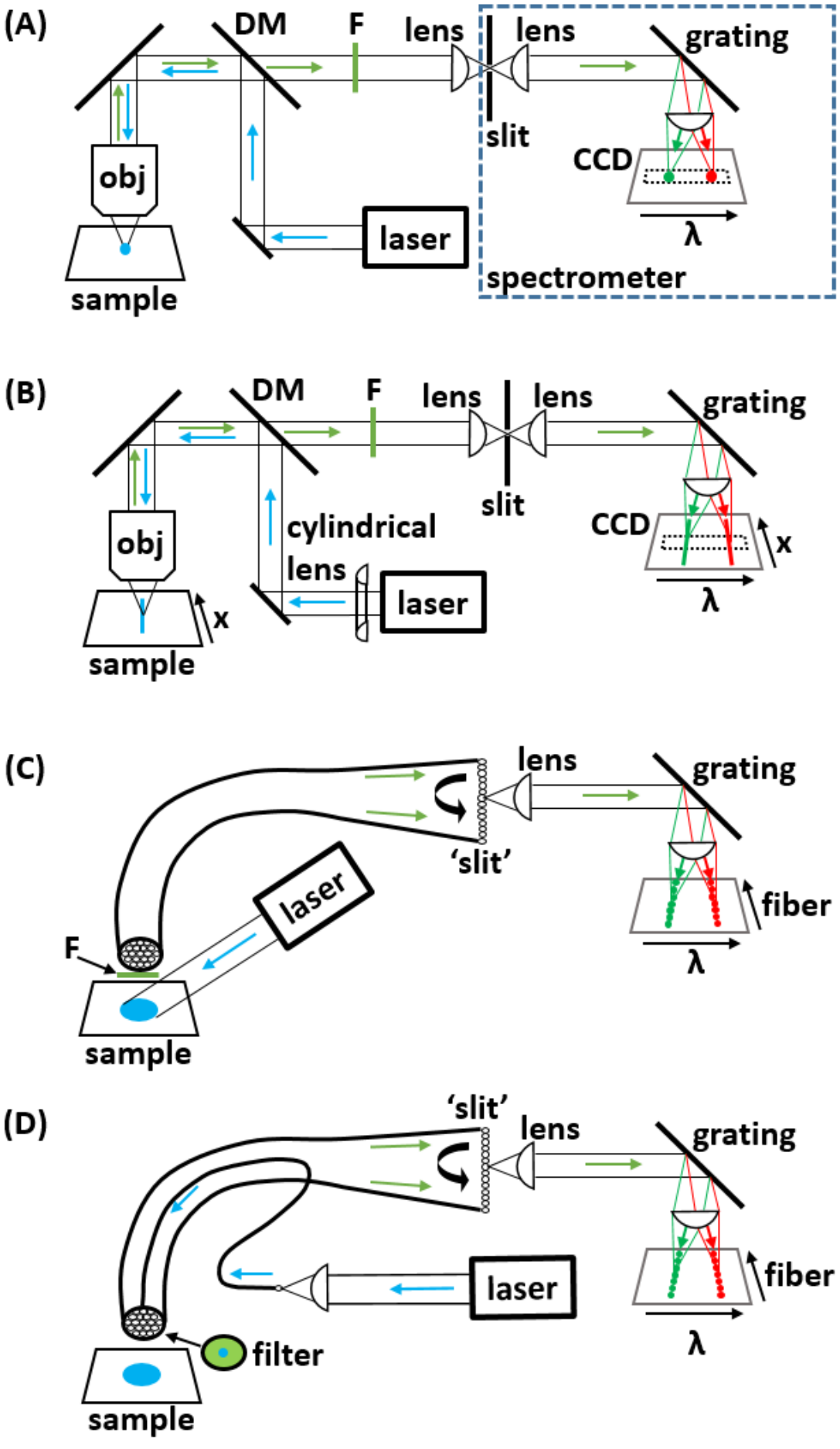
(A)
DM
F
lens
lens
grating
slit
CCD
obj
laser
λ
sample
spectrometer
(B)
DM
F
lens
lens
grating
slit
CCD
obj
cylindrical
lens
laser
x
x
λ
sample
(C)
lens
grating
'slit'
laser
fiber
F
λ
sample
(D)
'slit'
lens
grating
laser
fiber
filter
λ
sample

(E)

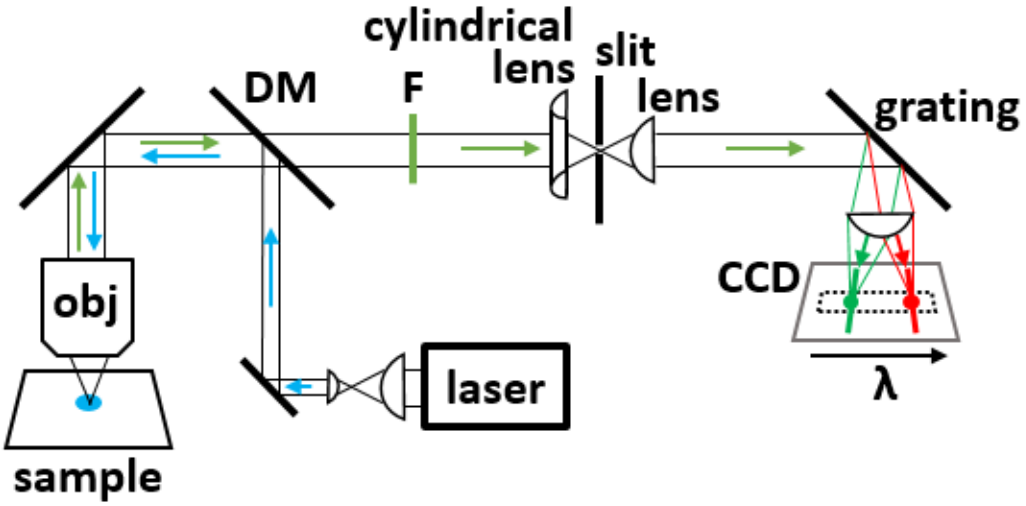
cylindrical lens
slit
DM
F
lens
grating
obj
CCD
laser
λ
sample

(F)

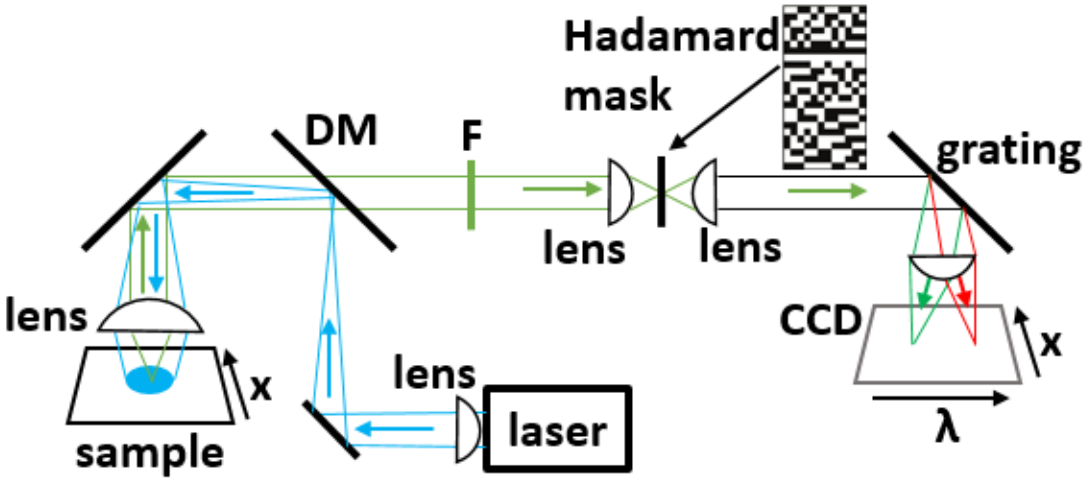
Hadamard mask
DM
F
grating
lens
lens
lens
CCD
x
lens
x
laser
λ
sample

(G)

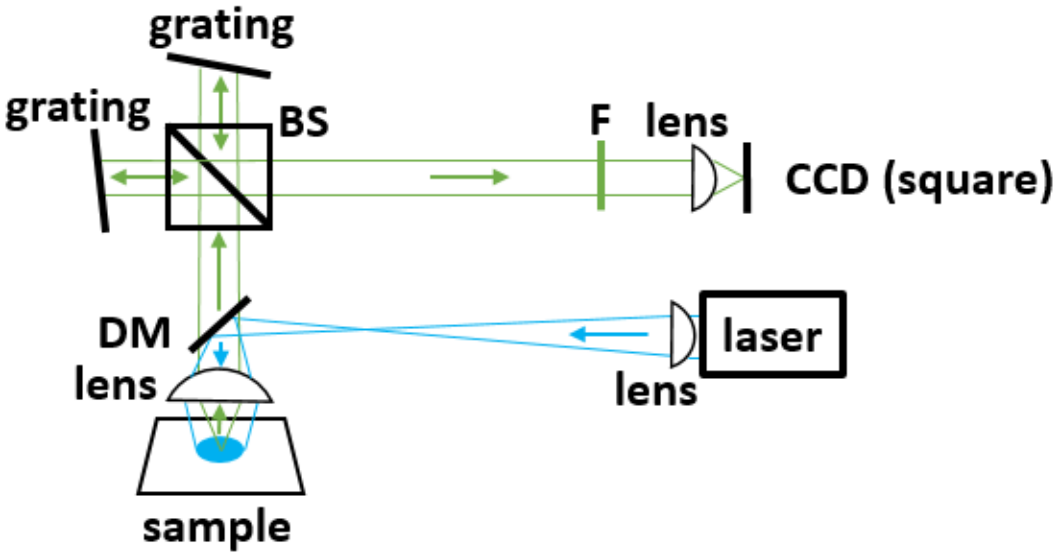
grating
grating
BS
F
lens
CCD (square)
DM
laser
lens
lens
sample

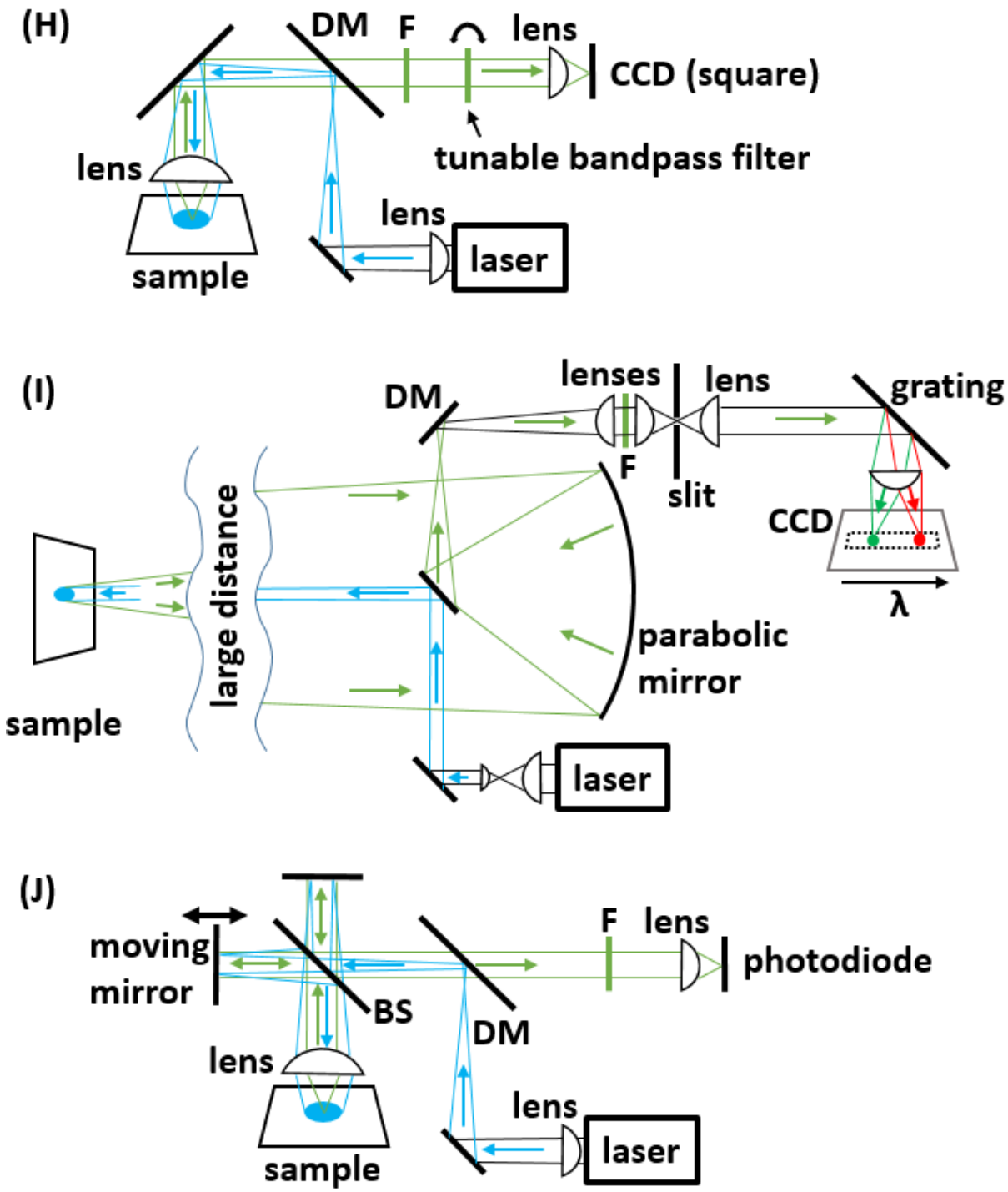

Figure 2. Various illumination and detection schemes for Raman spectroscopy are depicted. (A) Spot illumination, (B) Line illumination, (C) Circular to linear fiber bundle, (D) spatially offset Raman spectroscopy (SORS), (E) spot distortion, (F) Hadamard mask, (G) spatial heterodyne Raman spectroscopy (SHRS), (H) widefield imaging, (I) standoff detection, and (I) Fourier transform (FT-) Raman. Key: BS = (non-polarizing) beam splitter, CCD = charge coupled device, DM = dichroic mirror (long pass), F = long pass or notch filter, obj = objective lens. Laser light is depicted in blue, and Raman-scattered light in green.

3. Large area illumination Raman spectroscopy techniques

A. Spot illumination

This is the standard method for most Raman spectroscopy, and a schematic is shown in Figure 2(A). A laser spot is focused onto a sample and Raman-scattered light is collected using the same objective lens. A long pass dichroic mirror allows red-shifted light to pass through, but light from the laser is reflected towards the sample. This dichroic mirror also helps remove laser light reflected or scattered from the sample, and a notch or longpass filter ('F') removes more laser light. The collimated Raman beam is focused through a slit (with the length of the slit perpendicular to the drawing). The Raman light is then dispersed using a diffraction grating, then focused with a lens onto a CCD detector. Detected photons are 'binned' (or summed) perpendicular to the wavelength axis, in order to produce a spectrum. Using an objective lens with NA = 1.4 and assuming NA = 0.2 for the spectrometer, a magnification of 7 is achieved, so a Raman signal is collected from a spot diameter 7 times smaller than the slit width (100 µm / 7 ≈ 15 µm). This spot size is inserted into table 1 to deduce a spot area. The product of the spot area and the square of the NA of collection, is a measure of the expected signal level, to be used as a reference against other techniques presented in this section. Crucially this figure does not include increases in sampling depth which, except for schemes B and E, should greatly increase the signal level compared to spot illumination (whose sampling depth is around 10 µm for NA = 1.4 in collection).

B. Line illumination.

If a cylindrical lens is inserted into the laser path of the previous 'spot illumination' scheme, light will only be defocused in the axis of curvature of the cylindrical lens. In Figure 2(B), the laser beam is focused perpendicular to the plane of the schematic drawing, which is denoted as the 'x' axis. A line is formed, which must be within the field of view of a high numerical aperture lens. A recent objective lens (Olympus XLPlanN) has a good combination of high NA (1.05) and large field of view (around 0.5 mm). This NA gives a factor of 5 magnification, when compared to the spectrometer NA (≈0.2), so signal can be measured from a spot of diameter 20 µm – i.e. one-fifth of the spectrometer slit width. Using the cylindrical lens in one axis means a laser line of length 0.5 mm and width 20 µm can be projected onto the sample. This represents an improvement in signal levels for constant laser intensity at the sample, by a factor of 40 compared to spot illumination. Line illumination is mostly used for Raman imaging [8] : in this case the CCD detector is not binned, and each row on the CCD relates to a spectrum for a position in the sample along the line in the x axis.

C. Circular to linear fiber bundle.

Similar to the line illumination in Fig 2(B), a linear array of optical fibers in place of the slit also produces a set of spectra in rows on the detector. The line of fibers in Fig 2(C) has been rotated to aid visualisation, but during the measurement these fibers are aligned perpendicular to the page. In this case, the maximum number of fibers along the slit direction is limited by the height of the CCD chip. Common cooled CCD chips for spectroscopy are of the size 28 x 7 mm, which relates to 67 fibers of diameter 105 µm in a linear array. Without any magnification, this means that optical fibers with common NA of 0.22 are well matched to a f/2 spectrometer (NA≈0.24).

At the other end of the bundle, all fibers are arranged in a circle and positioned close to the sample. The diameter of this circle for 67 of these fibers is 1.0 mm, but the collection angle is only an NA of

0.22 for most multimode optical fibers. Higher NA fibers are available – up to 0.6 NA – but this would mean that the extra light collected into the fiber at higher angles wouldn't be accepted by the spectrometer with its lower NA. A filter – 'F' in Figure 2(C) – is required before the end of the fiber bundle, to prevent most of the laser from entering the fibers and generating an unwanted Raman signal from the glass.

The product of NA^2 and collection area (i.e. the overall signal level) is an order of magnitude higher than for line illumination. A commercial probe exists, using such a fiber bundle [9] albeit with a smaller NA of collection but a larger area of bundle, which allows the probe to be at a larger distance from the sample of interest.

D. Spatially Offset Raman Spectroscopy (SORS)

A similar method to that just described in part (C) is a spatially offset Raman probe – shown in Figure 2(D). The two schemes are identical, expect that in the case of SORS the laser is launched down the central fiber within the bundle. This makes the filter on the circular end of the bundle more complex – it needs a small central part to act as a short pass filter, to allow only the laser to pass but no Raman signal generated within the glass of the fiber. The outer part of the filter is as before: long pass to remove the laser light. Fabricating such a miniature filter is challenging but commercial probes exist in this format. This scheme results in the same effective area as the previous fiber bundle, but the probe can be placed closer to the sample and there is no need to focus the laser onto the region. When this probe is placed very close to the surface, most of the Raman signal which can enter the fibers is from regions deep beneath the surface. For this reason, this probe is highly advantageous when used for sub-surface analysis, such as *in vivo* diagnosis in tissues or blood vessels beneath the skin [10,11], and is used to analyse liquids within closed containers in airports [12].

E. Spot distortion

With spot illumination in Figure 2(A), a circular laser spot on the sample may be magnified in size when projected onto the spectrometer's slit, but still remains circular. In order to achieve a higher throughput, the circular spot at the input slit could be distorted so that it is stretched in the direction of the length of the slit and compressed along the width of the slit. This high throughput virtual slit [13-15] - depicted in Figure 2(E) - now uses the full area of the input slit, which relates to a larger area (and therefore radius) spot on the sample. The full area of the slit (7 mm x 0.1 mm) has an equal area to a circle of radius 0.84 mm, which if magnified by a factor of 7 (using a 1.4 NA objective lens) relates to a circle of radius 0.12 mm at the sample. The area of this spot on the sample is similar to that used by the fiber bundle techniques (C) and (D), as they also convert a circle into a shape to match the linear spectrometer input slit.

F. Hadamard mask

Hadamard spectroscopy [16-19] is a form of optical multiplexing. If the narrow slit at the input of a spectrometer is removed to leave a very large circular focused spot, it will blur out the sharp spectral peaks so they can longer be resolved. The circle projected onto the slit is first 'cut' horizontally into rows, and for a given row certain columns are masked, as shown in Figure 2(F). When spectra from each row are added or subtracted in a linear combination, the Raman spectrum of the source is

retrieved. The spectral widths of peaks are governed by the width of the pixels in the mask, and half the signal is absorbed by these masking pixels. Further noise, relative to a traditional slit-based spectrometer, is introduced into the detection because the signal from some rows is subtracted from the signal from other rows. Hence the overall improvement in signal levels is smaller than would be expected from the increase in spot area. Nevertheless, an improvement in signal levels of more than an order of magnitude was measured for a Hadamard mask spectrum of a Xenon lamp, compared to a slit-based spectrometer [20]. The ratio of areas in table 1 is more than 3 orders of magnitude, so it is clear that the Hadamard transform itself, along with other experimental issues, limits the signal-to-noise ratio achieved. A large diameter spot cannot be imaged by a high NA objective lens, so a large diameter achromatic lens would be employed instead, with an NA of around 0.4.

G. Spatial Heterodyne Raman Spectroscopy (SHRS)

Instead of using a long focal length spectrometer, spatial heterodyne spectroscopy uses diffraction gratings to disperse the light over a much shorter distance – as depicted in Figure 2(G). A beamsplitter is employed to coherently interfere Raman-scattered light, which produces a complex fringe pattern on a square CCD detector. If no magnification is required, the size of the spot on the sample can be as large as the cooled CCD camera – typically 13 mm. When the fringe pattern on the camera is put through a Fourier transform, it is converted to frequency space and a Raman spectrum is produced.

As noise from the entire detector gives rise to noise through the spectrum, this technique's signal-to-noise ratio is not quite as good as a standard dispersive spectrometer with spot illumination. For weakly scattering or weakly absorbing samples, as well as the increase in spot area, more of the signal is generated into the depth of the sample for SHRS compared to a dispersive system, so we would expect significantly higher signal levels for SHRS. The systems show a similar signal-to-noise ratio when using an order of magnitude more laser power for SHRS [20,21], which is equivalent to a reduction in signal-to-noise ratio by a factor of around 3. This suggests that the increase in signal from a larger depth is more than offset by the extra noise using this detection scheme, but still highlights the significant improvements likely with SHRS over slit-based spectrometers, when a constant laser intensity is used.

H. Widefield imaging

Although not strictly spectroscopy, widefield imaging has been used to acquire Raman images at specific wavenumbers. This scheme, shown in Figure 2(H) means illuminating a large area on the sample with the laser, and imaging directly onto a CCD camera with a bandpass filter tuned to one of the characteristic vibrational frequencies. Acquiring a Raman spectrum at each imaging pixel can be slow, so it makes sense to acquire images specific to bands within the spectrum, especially when the material in question has a small number of peaks at known frequencies. For example, when using the same laser intensity on a silicon sample, a widefield Raman imaging system – measuring the intensity of just the 520 cm^{-1} peak – achieved an order of magnitude improvement in signal-to-noise ratio compared to Raman imaging based on spot illumination, mainly due to reduced losses from the spectrometer [22]. The same article also compares these methods against line illumination for imaging. For spectroscopy of complex or organic systems with complex Raman spectra, images would be taken at a series of up to 100 different wavenumbers using an extremely narrow bandpass tunable filter, converted into a spectrum at each imaging pixel then averaged over the whole image. This would still be far quicker than methods (A)-(E), when laser intensity is limited in absorbing samples.

I. Standoff detection

In standoff detection, a very large distance (1 - 1500 m) is introduced between the sample and detector, usually for the purpose of detecting toxic, dangerous or inaccessible materials [23,24]. In order to have a hope of detecting a reasonable spectrum, a very large diameter lens would be used in a telescope arrangement. In reality, lenses over 20 cm in diameter are expensive, so reflective telescopes are preferred. A schematic is presented in Figure 2(I). The incident laser beam is collimated, tending to be several millimeters or more in diameter. Because the telescope has such a large focal length, it demagnifies the spot down to a spot far smaller than the maximum slit width of 100 µm for most spectrometers. A simple calculation reveals that the effective area in table 2 is independent of standoff distance, for a constant laser intensity on the sample.

J. FT-Raman

Before CCD detectors were developed, dispersive spectrometers would be scanned across a single small detector, and no multiplex advantage could be achieved by measuring all the spectrum simultaneously. So to give some multiplexing, Fourier Transform (FT-) Raman spectroscopy was developed. As depicted in Figure 2(J), Raman-scattered light is passed through a Michelson interferometer, and the length of one arm of the interferometer is gradually increased. The resulting interferogram with respect to time, is Fourier transformed into frequency space, and results in a Raman spectrum. In the early days of Raman spectroscopy, the high power of 1064 nm lasers was combined with near infra-red detectors, notably Germanium or Indium Gallium Arsenide (InGaAs), which both suffer from noise even at liquid nitrogen temperatures. However, a large area single detector can be used, so a large laser spot can be focused onto the sample. For the same laser intensity, FT-Raman was found to have a reduced signal-to-noise ratio by a factor of 5 compared to slit-based systems with CCD detectors [25]. Since the switch to CCD-based systems for lasers in the range 365 – 830 nm, almost all FT-Raman systems use 1064 nm lasers on samples which would suffer from high fluorescence with shorter wavelength laser excitation. The spot size is typically 1 mm, as a trade-off between laser-induced heating of the sample, and extra noise from an increasing detector size. One of the benefits of FT-Raman (and SHRS) is that the width of spectral peaks in the recovered Raman spectrum is not limited by the detector or pixel size. A FT-Raman study of gases [26] demonstrated a resolution of 0.02 cm^{-1}.

Conclusion

For samples with very low optical absorption, such as solvents and polymers, a spot illumination scheme is ideal for Raman spectroscopy. In such a scheme, laser light is focused to a diffraction limited spot. However, many sample types with moderate absorption are heated or damaged when the full laser power of up to 500 mW is focused into a micrometer-sized spot. Instead of simply reducing the laser power to avoid heating or damage, which would reduce the signal level proportionately, a number of alternative schemes are presented in table 1 aimed at increasing the area of illumination, so that a larger signal can be recorded.

For samples with higher absorption, an area of at least tens of square millimeters should be used. Three schemes fit this requirement, namely the Hadamard mask, spatial heterodyne Raman spectroscopy (SHRS) and widefield imaging. Hadamard mask spectroscopy and SHRS both have

increased noise compared to traditional Raman, but this degradation of the signal-to-noise ratio by around an order of magnitude is more than offset by 5-6 orders of magnitude increase in area of illumination. Widefield imaging would seem to be appropriate in cases where sample identification can be achieved with a small number of peaks, although noise is also increased compared to traditional Raman due to increased noise from across the whole detector. Specifically, for human tissue a maximum permissible exposure of 296 mW cm^{-2} and a 785 nm or 830 nm laser with 500 mW power output, only SHRS or widefield imaging schemes have an area large enough to benefit from the full laser power. After accounting for typical losses in laser power from optical components, this area is above a square centimeter.

For samples with relatively low absorption, an illumination area of the order of 0.01 mm^2 could be sufficient. In this case, the favored scheme is either line illumination or spot distortion. Both use a standard Raman system with a dispersive spectrometer, so maintain similar signal-to-noise levels as spot illumination. Spatially offset Raman spectroscopy (SORS) is only recommended when a signal from deep beneath the sample's surface is required.

Raman technique	Size of region on sample	Area on sample	Numerical aperture (NA) of collection	Area x NA^2 (≈ effective signal level)
A. Spot illumination	0.015 mm diameter	0.00018 mm^2	1.4	$3.5x10^{-4}$ mm^2
B. Line illumination	0.5 mm x 0.02 mm line	0.01 mm^2	1.05	0.01 mm^2
C. Circular-to-linear fiber bundle	Bundle diameter 0.8 mm (linear 0.105 mm x 7 mm)	0.5 mm^2	0.2	0.02 mm^2
D. Spatially Offset Raman Spectroscopy (SORS)	Bundle diameter 0.8 mm (0.105 mm x 7 mm at slit)	0.5 mm^2	0.2	0.02 mm^2
E. Spot distortion	0.17 mm diameter (ellipse 0.1 mm x 7 mm at slit)	0.02 mm^2	1.05	0.02 mm^2
F. Hadamard mask	7 mm diameter	38 mm^2	0.2	1.5 mm^2
G. SHRS	13 mm diameter	133 mm^2	0.4	21 mm^2
H. Widefield imaging	13 mm diameter	133 mm^2	0.4	21 mm^2
I. Standoff detection	diameter $8x10^{-5}$ x standoff distance (e.g. 8.3 mm for u = 100 m)	e.g. 55 mm^2 (u = 100 m)	e.g. $4.16x10^{-5}$ (u = 100 m)	10^{-7} mm^2
J. FT-Raman	1 mm diameter	0.7 mm^2	0.4	0.1 mm^2

Table 1. Comparison of various Raman spectroscopy techniques depicted in Figure 2. The size of the region on the sample is that which will pass through a 100 µm slit (A-E only). The numerical aperture (NA) of collection is highest for small spot which can benefit from an oil immersion objective lens with 1.4 NA. For larger spots up to 0.5 mm in diameter, a 1.05 NA objective lens is required. For spot sizes up to 13 mm, a large diameter achromatic lens with NA 0.4 is required. In these cases where the NA of collection is larger than the NA of the spectrometer (typically 0.2), a magnification of the spot is achieved. The last column represents the signal level achieved for a constant laser intensity on the sample. In this case, signal level is proportional to area, and to the solid angle of collection (which varies in a similar way to NA^2). However, this final column should also be adjusted for the sampling depth of the technique, and the signal-to-noise ratio of the detection technique. The latter depends on the detector type, number of pixels on the detector, the detection scheme (e.g. dispersed over large area vs. directed into small numbers of channels), and the type of spectrum (with a small number of sharp peaks or a large number of broad peaks). For standoff detection, u refers to the standoff distance between object and collecting mirror.

1 Raman, C. V. & Krishnan, K. S. A new type of secondary radiation. *Nature* **121**, 501 (1928).

2 Ryder, A. G., O'Connor, G. M. & Glynn, T. J. Quantitative analysis of cocaine in solid mixtures using Raman spectroscopy and chemometric methods. *Journal of Raman Spectroscopy* **31**, 221-227 (2000).

3 Allred, C. D. & McCreery, R. L. Near-infrared Raman spectroscopy of liquids and solids with a fiber-optic sampler, diode laser, and CCD detector. *Applied Spectroscopy* **44**, 1229-1231 (1990).

4 Weber, A., Porto, S. P., Cheesman, L. E. & Barrett, J. J. High-resolution Raman spectroscopy of gases with cw-laser excitation. *JOSA* **57**, 19-28 (1967).

5 Johansson, J. D. Spectroscopic method for determination of the absorption coefficient in brain tissue. *Journal of biomedical optics* **15**, 057005 (2010).

6 Senova, S. *et al.* Experimental assessment of the safety and potential efficacy of high irradiance photostimulation of brain tissues. *Scientific reports* **7**, 43997 (2017).

7 Lucas, J. F. & Hornef, J. Design and Calibration of a Raman Spectrometer for use in a Laser Spectroscopy Instrument Intended to Analyze Martian Surface and Atmospheric Characteristics for NASA. (2016).

8 Christensen, K. A. & Morris, M. D. Hyperspectral Raman microscopic imaging using Powell lens line illumination. *Applied spectroscopy* **52**, 1145-1147 (1998).

9 Shin, K. & Chung, H. Wide area coverage Raman spectroscopy for reliable quantitative analysis and its applications. *Analyst* **138**, 3335-3346 (2013).

10 Kong, K., Kendall, C., Stone, N. & Notingher, I. Raman spectroscopy for medical diagnostics—From in-vitro biofluid assays to in-vivo cancer detection. *Advanced drug delivery reviews* **89**, 121-134 (2015).

11 Ma, K. *et al.* In vivo, transcutaneous glucose sensing using surface-enhanced spatially offset Raman spectroscopy: multiple rats, improved hypoglycemic accuracy, low incident power, and continuous monitoring for greater than 17 days. *Analytical chemistry* **83**, 9146-9152 (2011).

12 Loeffen, P. W. *et al.* in *Optics and Photonics for Counterterrorism and Crime Fighting VII; Optical Materials in Defence Systems Technology VIII; and Quantum-Physics-based Information Security.* 81890C (International Society for Optics and Photonics).

13 Behr, B. *et al.* in *Applied Industrial Optics: Spectroscopy, Imaging and Metrology.* AM1B. 2 (Optical Society of America).

14 Gooding, E. A., Gunn, T., Cenko, A. T. & Hajian, A. R. in *Hyperspectral Imaging Sensors: Innovative Applications and Sensor Standards 2016.* 98600C (International Society for Optics and Photonics).

15 Gooding, E., Deutsch, E. R., Huehnerhoff, J. & Hajian, A. R. in *Biomedical Vibrational Spectroscopy 2018: Advances in Research and Industry.* 104900T (International Society for Optics and Photonics).

16 Nelson, E. & Fredman, M. Hadamard spectroscopy. *JOSA* **60**, 1664-1669 (1970).

17 Graff, D. K. Fourier and Hadamard: transforms in spectroscopy. *Journal of chemical education* **72**, 304 (1995).

18 McCain, S., Gehm, M., Wang, Y., Pitsianis, N. & Brady, D. Coded aperture Raman spectroscopy for quantitative measurements of ethanol in a tissue phantom. *Applied spectroscopy* **60**, 663-671 (2006).

19 Treado, P. J. & Morris, M. D. A thousand points of light: the Hadamard transform in chemical analysis and instrumentation. *Analytical chemistry* **61**, 723A-734A (1989).

20 Wagadarikar, A. A., Gehm, M. E. & Brady, D. J. Performance comparison of aperture codes for multimodal, multiplex spectroscopy. *Applied optics* **46**, 4932-4942 (2007).

21 Strange, K. A., Paul, K. C. & Angel, S. M. Transmission Raman measurements using a spatial heterodyne Raman Spectrometer (SHRS). *Applied spectroscopy* **71**, 250-257 (2017).

22 Schlücker, S., Schaeberle, M. D., Huffman, S. W. & Levin, I. W. Raman microspectroscopy: a comparison of point, line, and wide-field imaging methodologies. *Analytical chemistry* **75**, 4312-4318 (2003).
23 Carter, J. C. *et al.* Standoff detection of high explosive materials at 50 meters in ambient light conditions using a small Raman instrument. *Applied Spectroscopy* **59**, 769-775 (2005).
24 Aggarwal, R., Farrar, L. & Polla, D. Measurement of the absolute Raman scattering cross sections of sulfur and the standoff Raman detection of a 6-mm-thick sulfur specimen at 1500 m. *Journal of Raman Spectroscopy* **42**, 461-464 (2011).
25 Dzsaber, S. *et al.* A Fourier transform Raman spectrometer with visible laser excitation. *Journal of Raman Spectroscopy* **46**, 327-332 (2015).
26 Bendtsen, J. High-resolution Fourier transform Raman spectra of the fundamental bands of 14N15N and 15N2. *Journal of Raman Spectroscopy* **32**, 989-995 (2001).